Liquid Crystals
Publication details, including instructions for authors and subscription information:
http://www.informaworld.com/smpp/title~content=t713926090

Thickness dependent low frequency relaxations in ferroelectric liquid crystals with different temperature dependence of the helix pitch

V. Novotna; M. Glogarova; A. M. Bubnov; H. Sverenyak

Online publication date: 11 November 2010

To cite this Article Novotna, V. , Glogarova, M. , Bubnov, A. M. and Sverenyak, H.(1997) 'Thickness dependent low frequency relaxations in ferroelectric liquid crystals with different temperature dependence of the helix pitch', Liquid Crystals, 23: 4, 511 — 518
To link to this Article: DOI: 10.1080/026782997208091
URL: http://dx.doi.org/10.1080/026782997208091

LIQUID CRYSTALS, 1997, VOL. 23, NO. 4, 511–518

Thickness dependent low frequency relaxations in ferroelectric liquid crystals with different temperature dependence of the helix pitch

by V. NOVOTNÁ, M. GLOGAROVÁ*, A. M. BUBNOV and H. SVERENYÁK
Institute of Physics, Academy of Sciences of the Czech Republic, Na Slovance 2, 180 40 Prague 8, Czech Republic

(*Received 31 January 1997; in final form 28 April 1997; accepted 5 May 1997*)

A low frequency relaxation mode 1 has been detected in ferroelectric phases of three materials. The relaxation frequency and the dielectric strength of this mode depend strongly on the sample thickness, but their temperature dependences are qualitatively different in the materials studied, reflecting the behaviour of the helicoidal structure of these materials. This mode has been attributed to a superposition of the Goldstone and thickness modes when the helicoidal structure exists and to the thickness mode only, when the helix is unwound. In addition, with one material, mode 2 has been detected at still lower frequencies, and this also exhibits a strong sample thickness dependence. It was attributed to fluctuations of the director field modified by a non-homogeneous ionic charge distribution across the sample. As both modes 1 and 2 are strongly sample thickness dependent, they do not represent bulk properties of the materials studied, but reflect the structure in real samples, which is determined by surface conditions.

1. Introduction

In the ferroelectric chiral smectic C (SmC*) phase two low frequency modes exist, the soft and Goldstone modes, which are connected with the structural change at the SmA→SmC* phase transition. This change, namely the tilting of molecules from the smectic layer normal, is described by a 2-dimensional parameter [1] $\xi_1 = \theta \sin \phi z$, $\xi_2 = \theta \cos \phi z$, where θ denotes the amplitude and ϕ the phase of the mean molecular tilt from the layer normal (z-axis). The soft mode represents the fluctuations $\delta\theta$, and the Goldstone mode, existing due to the breaking of the continuous symmetry, represents the phase fluctuations $\delta\phi$. As the local optical axis is parallel to the mean molecular long axis (director), both modes can be detected in the electro-optical response. The electro-optical response of the soft mode in the SmA phase is known as the electroclinic effect [2]. Due to a linear interaction of the order parameter with the polarization, both modes can be seen in the dielectric response as well. These two modes describe completely the low frequency dynamics of the SmC* phase in ideal infinite samples. It is well known that in the SmC* phase the soft mode can be detected only near the SmA→SmC* phase transition and when the Goldstone mode is suppressed by a d.c. biasing field. Otherwise it is overwhelmed by the Goldstone mode.

*Author for correspondence.

The relaxation frequency f_G and the dielectric strength $\Delta\varepsilon_G$ of the Goldstone mode [1] depend on the helix pitch length p, being

$$f_G = 4\pi^2 K/\gamma p^2 \tag{1a}$$

$$\Delta\varepsilon_G = \varepsilon_0 \kappa^2 C^2 p^2/8\pi^2 K \tag{1b}$$

where K represents the elastic constants, γ is the viscosity, ε_0 is the dielectric constant of a vacuum, κ is the high temperature dielectric susceptibility (temperature independent), and C is the linear coupling constant between the tilt and polarization. When the coupling between the tilt and polarization is non-linear, which is the case far from the phase transition to the SmC* phase,

$$\Delta\varepsilon_G \approx (1/8\pi^2 K)(p\mathbf{P}_s/\theta_s)^2, \tag{2}$$

where $\mathbf{P}_s$ and θ_s are the spontaneous polarization and tilt angle [3].

The situation in real finite samples is much more complicated, and besides the soft and Goldstone modes, other low frequency relaxation processes have been reported. In materials with a very high spontaneous polarization, $\mathbf{P}_s$, two domain modes have been found [4, 5], which have been attributed to a formation of surface and bulk ferroelectric domains. The domains are formed under the application of a d.c. electric field in order to compensate the high local dipole moments

0267–8292/97 $12·00

which arise because the helix is suppressed [5]. The dielectric strength of the domain modes is much lower than that of the Goldstone mode, the relaxation frequencies of the bulk and the surface domain modes being around 1 and 10 kHz, respectively [5].

A weak mode with a relaxation frequency of a few kHz has been reported [6], and this has been related to a defect structure with different directions of the helical axis in poorly aligned planar samples. Another weak relaxation has been recognized in the ferroelectric SmC* phase; this has a high $\mathbf{P}_s$ around several kHz, but its origin has not been identified [7].

At frequencies <1 Hz, a very strong mode has been found which has not been attributed to a vibration of the molecular structure, but to the space charge accumulated on interfaces between the liquid crystal and the polyimide layer that is coated on the glass surfaces to ensure planar anchoring [8].

When planar samples, with the smectic layers perpendicular to the sample plane (book shelf geometry), are sufficiently thin, the helix is suppressed by surface interactions [9] and therefore the Goldstone mode does not exist. In such samples, two types of structures can occur, depending on the anchoring on the sample surfaces. The *homogeneous structure* arises when the molecules, as well as the directions of the local $\mathbf{P}_s$, are parallel on both surfaces. Such a structure occurs in very thin samples ($\approx 1\,\mu$m) or in samples with only slightly polar surface anchoring. The dielectric response of this structure has been investigated in [10], where it was established that both the relaxation frequency and dielectric strength of the response are thickness dependent as given by $f_r \sim 1/d^2$ and $\Delta\varepsilon \sim d$, respectively, d being the sample thickness. When the surface anchoring is strongly polar, which is usually the case in chiral smectics, the molecular long axes at the opposite sample surfaces make an angle $2\theta_s$ and the $\mathbf{P}_s$ vectors are antiparallel. This configuration results in in-smectic-layer director twist–bend and the $\mathbf{P}_s$ vector splays along the sample plane normal [11]. This structure has been called a *twisted structure*. A contribution of the fluctuations of the twisted structure ('thickness mode' [12]) to ε is very high, comparable to the contribution of the Goldstone mode in helicoidal samples. The dielectric strength as well as the relaxation frequency of the thickness mode are strongly dependent on the sample thickness, approximately as $\Delta\varepsilon_{th} \sim d^2$ and $f_{th} \sim 1/d^2$ [12]. A thickness dependent dielectric strength and relaxation frequency have also been reported in [13], but without an interpretation connected to the sample structure.

The director twist–bend accompanied with the splay of the $\mathbf{P}_s$ vector exists also in normal thick samples, in which the helix is well developed. When studying either dielectric or electro-optic response in the SmC* phase in these samples, the Goldstone mode and the thickness mode are indistinguishable, probably because both modes exhibit their relaxations in the same frequency region.

With ferroelectric (FE) liquid crystals exhibiting a high $\mathbf{P}_s$, a structure with the unwound helix can exist even in rather thick samples ($\sim 100\,\mu$m). In these materials the dechiralization lines, which inevitably accompany the helix, would have very high energy because they possess a relatively high bound charge [12]. Another reason for the unwinding of the spontaneous helical twist exists with substances exhibiting a spontaneous helical twist inversion at a certain temperature T_i in the SmC* phase [14]. In these materials, the helix pitch increases to infinity when approaching T_i, which ensures spontaneous helix unwinding over a broad temperature range around T_i in samples of a finite thickness. In this temperature range the Goldstone mode does not exist and the thickness mode can be detected separately [15].

In the present paper we study the dielectric and electro-optic dispersion in three FE liquid crystalline materials of similar chemical composition, with different temperature dependence of the helix pitch in samples of different thickness. This study contributes to an understanding of the behaviour of both the Goldstone and the thickness modes. In addition, we study the origin of a very low frequency mode, which we have found during a preliminary study [15] in the material exhibiting the helix twist inversion phenomenon [16]. This mode seems to be different from any of the modes reported so far by other authors and mentioned above.

2. Experimental

The liquid crystal materials used were

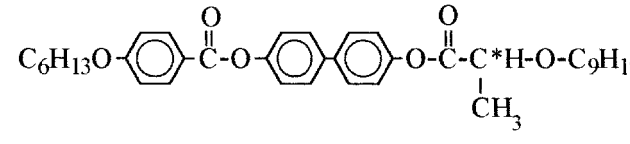

denoted as **H6/9**, which exhibits the phase sequence [16] Cr–25°C–SmC*–124°C–SmA–128°C–N*–136°C–BP–137°C–I and gives helix twist inversion, with the inversion temperature $T_i = 99$°C, together with two other substances of the general formula

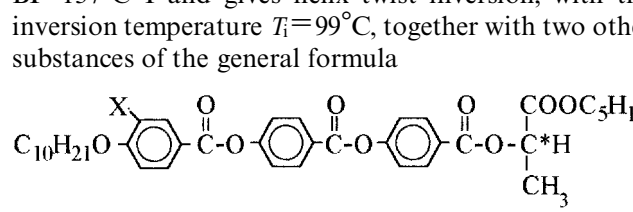

Here X stands for H or Cl; the latter two substances are denoted as **10AL** or **10ALCL**, respectively, with the phase sequences [17] Cr–35°C–SmC*–83°C–SmA–

141°C–I for **10AL** and Cr–36°C–SmC*–71°C–N*–96°C–I for **10ALCL**.

The samples were filled into cells composed of glass plates provided with ITO transparent electrodes and polyimide layers unidirectionally rubbed, which ensures planar (book shelf) geometry. The sample thickness d was defined by mylar sheets—6, 12, 25, 50, and 100 μm. The sample alignment was improved by using an electric field of 10 to 20 Hz, 40 kV cm^{-1} applied for 10 to 60 min. During measurements, the alignment was checked using a polarizing microscope. No zig-zag defects were observed in samples of any thickness. This finding implies that the layer structure in the samples does not exhibit chevrons, probably due to rather weak surface anchoring. From the sample texture one can also discern the spatial modulations in the sample. The texture is decorated by dechiralization lines, the spacing of which is equal to the helicoidal pitch. The twisted structure is confirmed by the rotation of the plane of polarized light by $2\theta_s$ on passing through the sample, where θ_s is the tilt angle.

We measured the frequency dispersion of the complex permittivity by using a Schlumberger 1260 impedance analyser in the frequency range of 10 Hz to 1 MHz, keeping the temperature of the sample stable within ±0·1 K. The temperature could be gradually lowered in steps of 1·5 to 2 K, smaller steps being used just below the phase transition T_c to the SmC* phase. With the sample of 25 μm thickness, the electro-optic response was measured in the frequency range of 10 Hz to 100 kHz as the real and imaginary parts of the light transmitted through the sample when an electric field was applied. The helix pitch was measured by diffraction studies using He-Ne laser light. The results of the dielectric study are not sensitive to disorientation in the sample plane (fan shaped texture), because the permittivity is isotropic in this plane. On the other hand, for the electro-optic work, perfect alignment is necessary.

3. Experimental results

Frequency dependences of the imaginary part of the permittivity (ε'') for the 25 μm thick sample of **H6/9** are shown in figure 1 (*a*) for selected temperatures. They exhibit two relaxation processes denoted mode 1 and mode 2, which are clearly seen as two maxima in the $\varepsilon''(f)$ dependences (see figure 1 (*a*)). Both these modes are also detectable in the frequency dispersion of the electro-optic response. The $\varepsilon''(f)$ dependences measured for **10AL** and for **10ALCL** (figures 1 (*b*) and 1 (*c*), respectively) show only one mode. Under an applied electric bias field mode 1 is suppressed.

The frequency dispersion data were analysed using

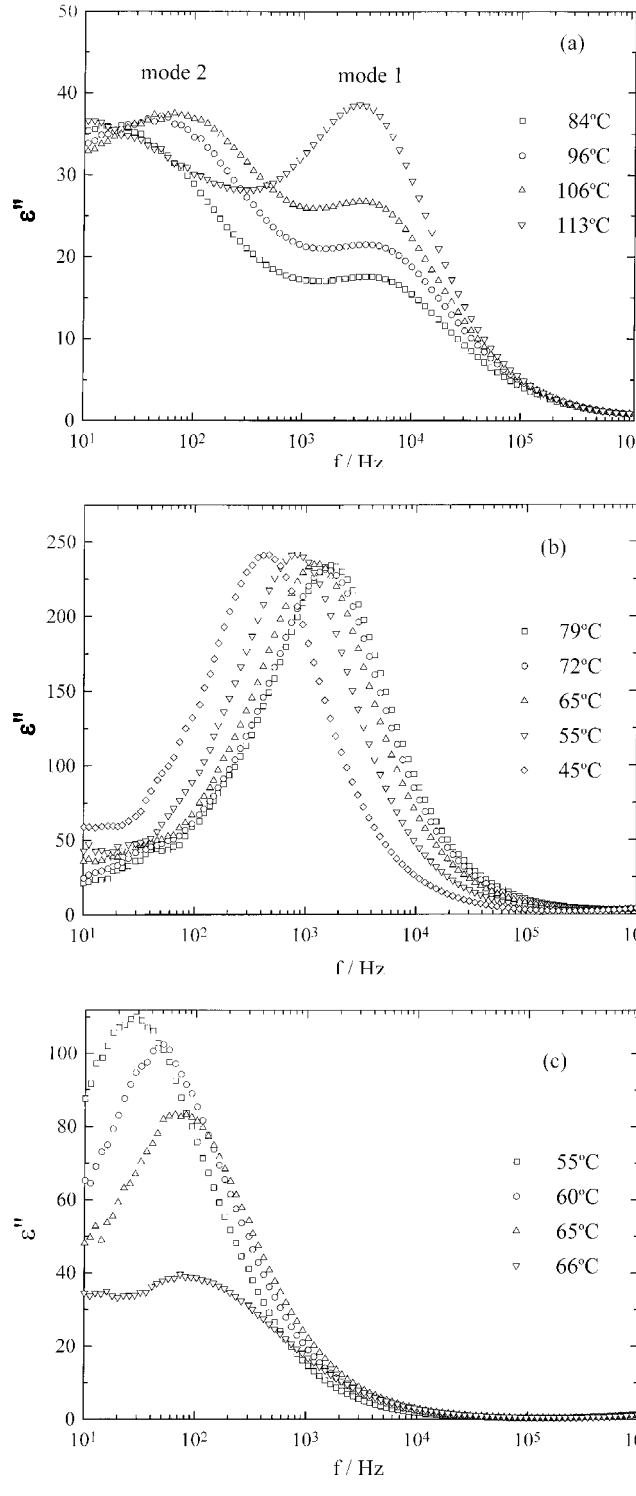

Figure 1. Frequency dispersion of the imaginary part of the permittivity ε'' measured for 25 μm thick samples at the indicated temperatures (*a*) **H6/9**, (*b*) **10AL**, (*c*) **10ALCL**.

the Cole–Cole formula:

$$\varepsilon^* - \varepsilon_\infty = \frac{\Delta\varepsilon_1}{1+(\mathrm{j}f/f_1)^{(1-\alpha_1)}} + \frac{\Delta\varepsilon_2}{1+(\mathrm{j}f/f_2)^{(1-\alpha_2)}} \qquad (3)$$

where f_1, f_2, $\Delta\varepsilon_1$, $\Delta\varepsilon_2$, and α_1, α_2 are the relaxation frequencies, dielectric strengths and distribution parameters for modes 1 and 2. The relaxation frequencies f_1, f_2 were determined by fitting the imaginary part of equation (3); the dielectric strengths $\Delta\varepsilon_1$, $\Delta\varepsilon_2$, as well as parameters α_1, α_2 were determined from the Cole–Cole plot $\varepsilon''(\varepsilon')$. For **10AL** and **10ALCL**, where only one relaxation peak has been observed in $\varepsilon''(f)$, only the first term in equation (3) has been used.

The temperature dependences of the fitted f_1 and $\Delta\varepsilon_1$ for any of the sample thicknesses studied are shown in figures 2(*a*) and 2(*b*), 3(*a*) and 3(*b*), and 4(*a*) and 4(*b*), for **H6/9**, **10AL** and **10ALCL**, respectively. Pronounced thickness dependences of both quantities are seen over the whole temperature regions studied. The values of the parameters α_1 are in the range 0·08 to 0·12 independent of the sample thickness. The low values of α_1 give evidence for a nearly monodispersive character of mode 1. At low temperatures, f_1 could not be evaluated because a maximum in $\varepsilon''(f)$ did not occur; this happened especially for the samples with low relaxation frequencies. The reason was either a rather high value of the ionic conductivity in these samples, which exceeded the imaginary part of the permittivity at low frequencies or, with **H6/9**, a merging of both modes 1 and 2 for thick samples. In these cases $\Delta\varepsilon_1$ too was not evaluated.

Figure 5 shows the thickness dependences of f_1 and $\Delta\varepsilon_1$ for **H6/9** at a constant temperature. For **10AL** and **10ALCL** the dependences are qualitatively the same. In all materials studied, the relaxation frequency f_1 increases remarkably with diminishing cell thickness; the dielectric strength $\Delta\varepsilon_1$, on the contrary, very steeply decreases. For mode 2, detected for **H6/9** only, f_2 increases and $\Delta\varepsilon_2$ decreases with decreasing sample thickness, similarly to mode 1. The value of $\alpha_2 = 0{\cdot}4$ to 0·5 shows a polydispersive character of mode 2.

The temperature dependences of the helix pitch are shown in figures 6(*a*) and 6(*b*) for **H6/9** and **10AL**, respectively. For **H6/9**, the pitch length increases with decreasing temperature down to about 114°C. Below this temperature the diffraction pattern disappears as the helicoidal structure becomes completely unwound in the whole sample. Microscopic observation shows that the unwinding process is not regular with increasing pitch, but when approaching full unwinding on cooling, the helix becomes unwound in some parts of the sample, the area of which then gradually increases. The thinner the sample, the higher temperatures where unwinding appears. The 12 μm thick sample becomes unwound even below 117°C, and the sample of $d = 6$ μm is unwound over the whole temperature range of the SmC* phase, because its $d \approx p$ [11]. In samples with the helix unwound, there exists a modulation along the sample plane normal, which is seen, using crossed polarizers, as a rotation of the polarized light plane by $2\theta_s$, where θ_s is the tilt angle. In the samples of **10AL** and **10ALCL** of $d = 6$ μm, the helicoidal structure exists because of its short pitch (see figure 6(*b*) for **10AL**). Compound **10AL** shows an increase of the pitch length in a narrow temperature range just below the SmA–SmC* phase transition temperature. On further cooling the pitch remains constant down to crystallization. The pitch of **10ALCL** is significantly shorter (about 0·6 μm) and for this reason it is not possible to measure it precisely by laser light diffraction. The dechiralization lines decorating the helicoidal texture cannot be seen because their spacing is below the resolution of the optical microscope. Under a low bias field, the line spacing is increased and the lines become visible in the microscope. When the line spacing is high enough under the applied field, a rotation of the polarized light plane by $2\theta_s$ can be detected between the lines, which indicates the existence of the twisted structure in these samples.

4. Discussion and conclusions

In the dielectric response of **H6/9** two modes (1 and 2) have been found in the SmC* phase; these have also been detected in the frequency dispersion of the electro-optic effect. This fact establishes that both modes are director vibrations. In **10AL** and **10ALCL**, only mode 1 has been detected. The reason might be the low temperature of the SmC* phase in these substances, which decreases the relaxation frequencies of both modes 1 and 2. Then the very low frequency dispersion of mode 2 could be hidden in the conductivity contribution.

Mode 1 is easily suppressed by a bias field, which is a typical behaviour of the Goldstone mode, based on the existence of the helical structure. On the other hand, mode 1 exists even in the temperature range where the helix is spontaneously unwound due to the helix twist inversion phenomenon or in 6 μm thick samples of **H6/9**, where the helix is unwound within the whole SmC* phase due to surface interactions [9, 11]. Moreover, the relaxation frequency f_1, as well as the dielectric strength $\Delta\varepsilon_1$, are strongly thickness dependent.

When the helicoidal structure is unwound, mode 1 can be attributed to the thickness mode (fluctuations of the director twist–bend along the sample plane normal) [12]. If the helicoidal structure is present in the sample, the twist–bend deformation also exists, producing a space modulation along the sample plane normal, i.e. in the direction perpendicular to the helix axis. In such samples both the Goldstone and the thickness modes contribute to the dielectric, as well as to the electro-optic response. The coexistence of the Goldstone and the thickness modes can be demonstrated through the temperature dependences of the dielectric strength of

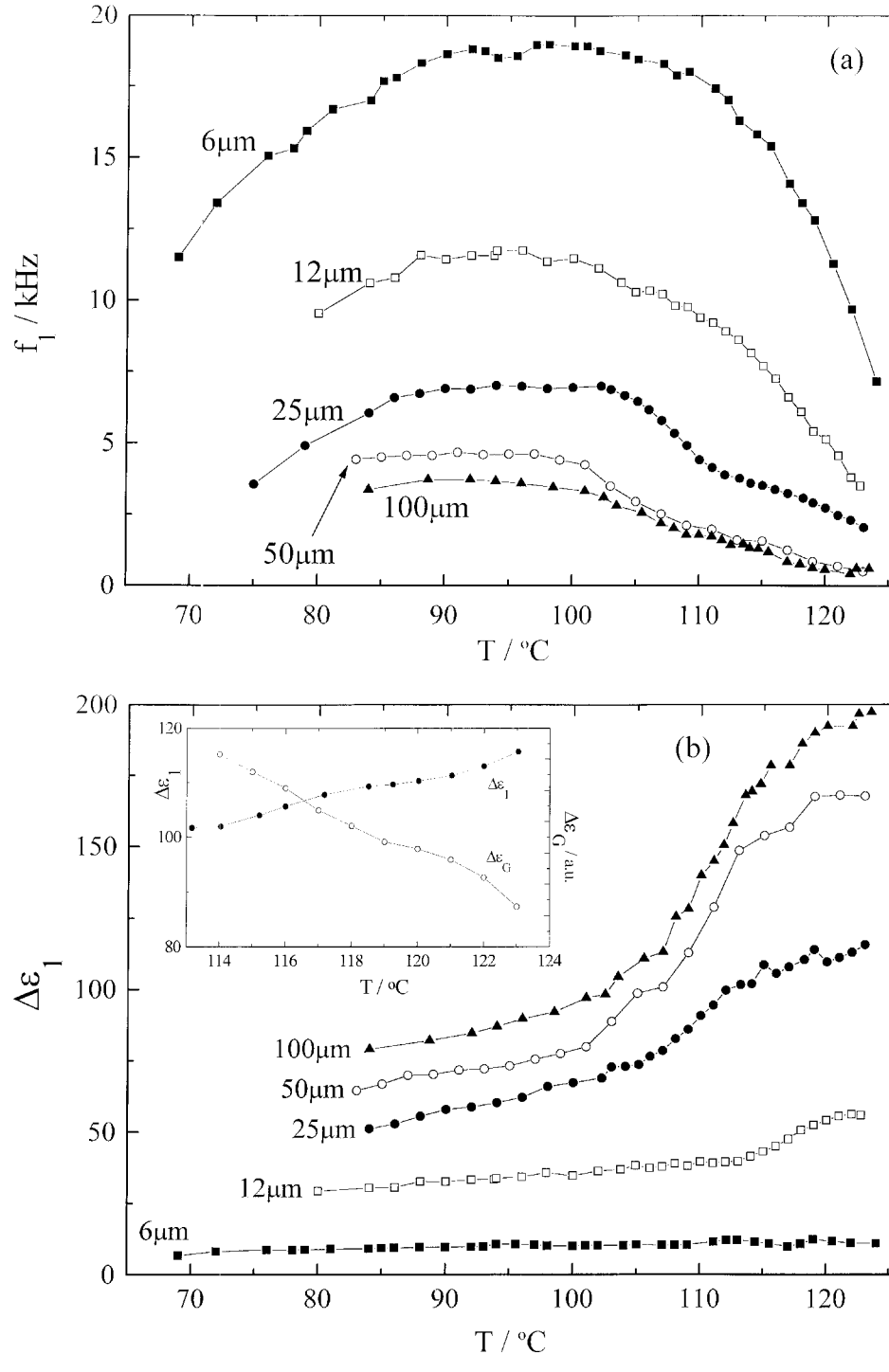

Figure 2. Temperature dependences of (*a*) the relaxation frequencies f_1 and (*b*) the dielectric strengths $\Delta\varepsilon_1$ of mode 1 for **H6/9** samples of different thickness. In the inset there is a comparison of the measured $\Delta\varepsilon_1$ with the Goldstone mode contribution to the dielectric constant $\Delta\varepsilon_G$, calculated (in relative units) from equation (2) using measured $p(T)$, $\mathbf{P}_s(T)$, and $\theta_s(T)$ dependences and arbitrary K, temperature independent; the comparison is done for the 25 μm thick sample and in the temperature range where the helix exists.

mode 1 (see figures 2(*b*), 3(*b*), and 4(*b*)), as will be discussed below.

For **H6/9**, at temperatures where the helicoidal structure is present, both (Goldstone and thickness) modes contribute to $\Delta\varepsilon_1$, which results in high values of $\Delta\varepsilon_1$ (except for the 6 μm thick sample, which is unwound in the whole SmC* phase). When approaching an unwinding temperature from above, $\Delta\varepsilon_1$ decreases steeply. This fact agrees with the microscopic observations showing that the sample area with the helicoidal structure, which produces the Goldstone mode contribution, decreases.

The 12 μm thick sample becomes completely unwound even below 117°C, which is reflected in the drop in $\Delta\varepsilon_1$

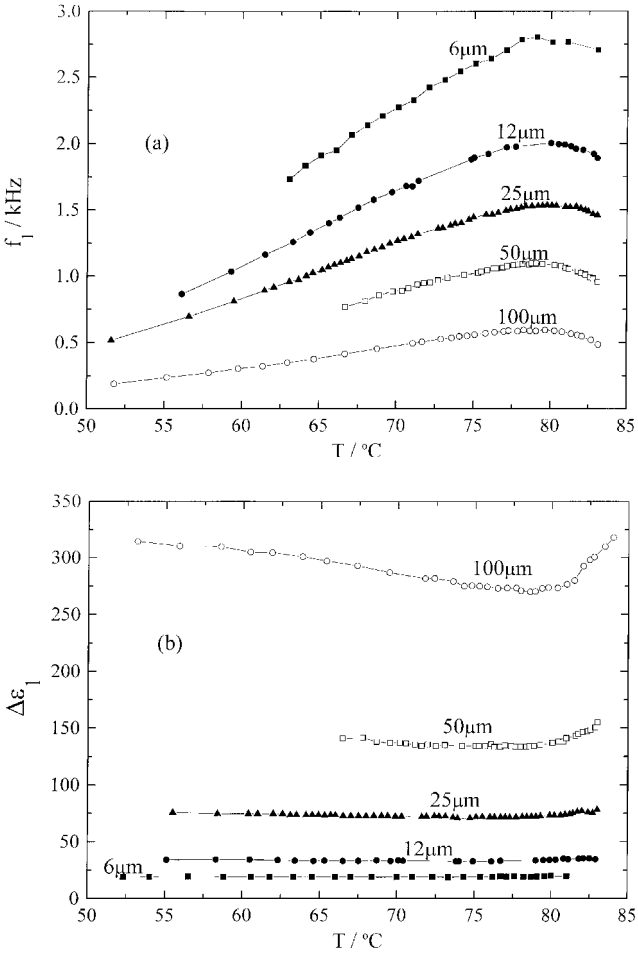

Figure 3. Temperature dependences of (*a*) the relaxation frequencies f_1 and (*b*) the dielectric strengths $\Delta\varepsilon_1$ of mode 1 for **10AL** samples of different thickness.

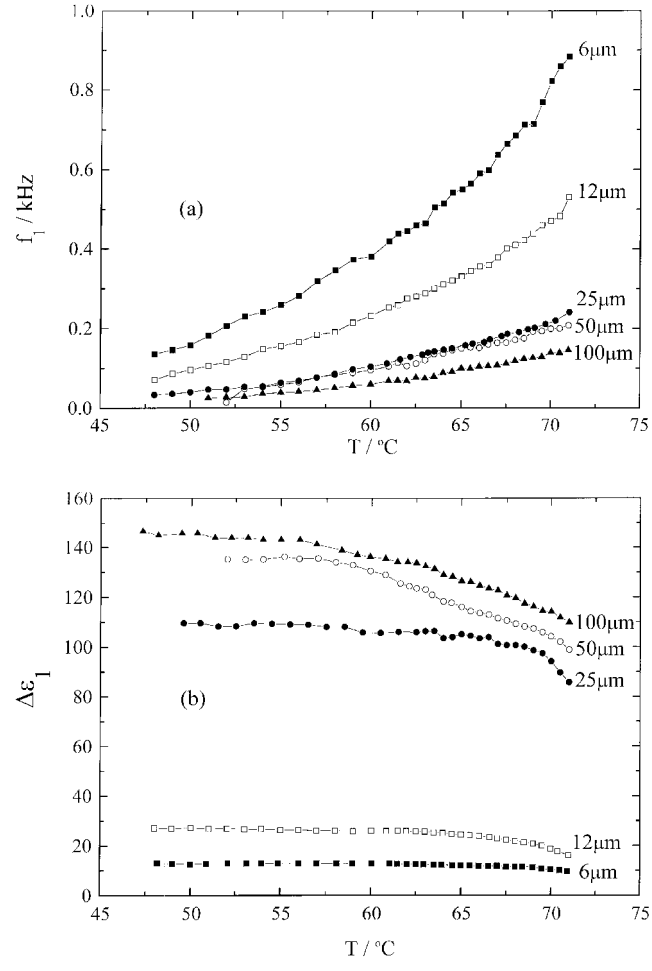

Figure 4. Temperature dependences of (*a*) the relaxation frequencies f_1 and (*b*) the dielectric strengths $\Delta\varepsilon_1$ of mode 1 for **10ALCL** samples of different thickness.

below this temperature (see figure 2 (*b*)). On the low temperature side of the SmC* phase, $\Delta\varepsilon_1$ arises from the thickness mode only, because the sample remains unwound down to the occurrence of crystallization. The remarkable thickness dependence of $\Delta\varepsilon_1$ over the whole temperature region is due to the strong thickness dependence of the thickness mode [12], which is still present for the whole SmC* phase region.

The temperature dependence of the relaxation frequency f_1 of **H6/9** (see figure 2 (*a*)) exhibits an increase on cooling below the SmA–SmC* phase transition, which is more evident for thin samples; then there is a constant part, followed by a slight decrease at low temperatures. Let us point out that the strong increase of f_1, as well as the decrease of $\Delta\varepsilon_1$ just below T_c, cannot be explained by the temperature dependence of the Goldstone mode contribution due to the pitch variation (see equations (1 *a*) and (1 *b*)). For p increasing on cooling below T_c (see figure 6 (*a*)), $\Delta\varepsilon_G$ should increase and

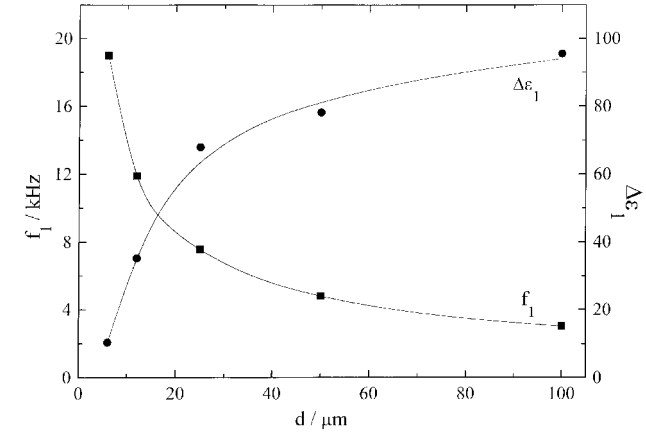

Figure 5. Thickness dependences of f_1 and $\Delta\varepsilon_1$ determined for **H6/9** at $T = 90°C$. The lines represent only a guide for the eye.

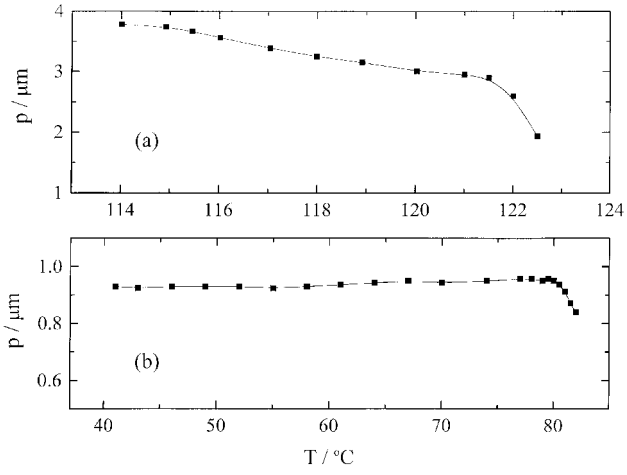

Figure 6. Temperature dependences of the helix pitch for (*a*) **H6/9**, 25 μm thick sample and (*b*) **10AL**, 50 μm thick sample.

f_G decrease, which is exactly contrary to the $\Delta\varepsilon_1(T)$ and $f_1(T)$ dependences experimentally found (cf. figures 2(*a*) and 2(*b*)). The non-linear interaction between $\mathbf{P}_s$ and θ_s, which can modify the temperature dependence of $\Delta\varepsilon_G$ (see equation (2)), cannot reverse the situation as this interaction is expected to be weak near T_c. The situation is demonstrated in the inset of figure 2(*b*), where the temperature dependence of $\Delta\varepsilon_G$ calculated from equation (2) is compared to the measured $\Delta\varepsilon_1$. The temperature dependences of $\Delta\varepsilon_1$ found just below T_c could be explained qualitatively by a gradual extinction of the Goldstone mode because of the helix unwinding on cooling. As for f_1, its increase on cooling just below T_c is probably driven by the temperature dependence of the thickness mode, which is seen on the $f_1(T)$ curve for the 6 μm thick sample, where only the thickness mode contributes to the dielectric response. The low temperature decrease of f_1 might be caused by an increase in viscosity.

For **10AL**, only mode 1 has been detected. This material does not exhibit the helix twist inversion phenomenon, so that the helix is present over the whole temperature range of the SmC* phase, which is true even for the 6 μm thick sample. Both the thickness and Goldstone modes are present and influence the dielectric properties. Just below T_c, f_1 increases and $\Delta\varepsilon_1$ decreases on cooling. Due to the pitch variations observed in this temperature region (see figure 6(*b*)), both quantities corresponding to the Goldstone mode would exhibit exactly opposite temperature dependences (cf. equations (1*a*) and (1*b*)). Similarly to **H6/9**, the non-linear interaction between $\mathbf{P}_s$ and θ_s cannot significantly affect $\Delta\varepsilon_G$ values near T_c. The observed temperature dependences in the narrow temperature range below T_c are probably caused by the temperature dependence of the thickness mode contribution, similarly to **H6/9**. At lower temperatures, $\Delta\varepsilon_1$ is nearly temperature independent for each thickness, but f_1 decreases with decreasing temperature, probably due to the increase of viscosity.

We can expect that for **10ALCL**, the helicoidal structure exists in all samples studied, similarly to **10AL**, because the inequality $d \gg p$ is valid. Thus both the Goldstone and thickness modes are present.

The dielectric properties of **10ALCL** differ significantly from those determined for **H6/9** and **10AL**, namely below T_c, where both f_1 and $\Delta\varepsilon_1$ exhibit opposite temperature dependences (see figures 4(*a*) and 4(*b*)) compared with **H6/9** and **10AL**. Unfortunately, the effect of the pitch behaviour on these quantities cannot be studied as the temperature dependence of the helix pitch length could not be measured because of its extremely low value. Besides, a plausible theoretical description of dielectric properties in the vicinity of the N*–SmC* phase transition is still not available.

In the determination of $\Delta\varepsilon_1$, a systematic error can arise for samples which exhibit a very low relaxation frequency f_1, because the permittivity is strongly exceeded by the ionic conductivity contribution at low frequencies. This might be the reason why the values of $\Delta\varepsilon_1$ are found to be higher than expected for the 100 μm thick sample of **10AL** and for the 25, 50 and 100 μm thick samples of **10ALCL**. The fitting procedure does not affect significantly the temperature dependences.

Generally, one can conclude that in helicoidal samples, mode 1 can be interpreted neither as the Goldstone mode, nor the pure thickness mode, but as a superposition of both modes. In twisted samples, i.e. in the temperature region where the helix is unwound due to helix twist inversion, or in 6 μm thick samples of **H6/9**, mode 1 represents just the thickness mode. Experiment shows that in both helicoidal and twisted samples, the mode 1 relaxation frequency varies by a factor of 5 to 10 (for different materials) when the sample thickness is changed from 6 to 100 μm. With all three compounds studied, the observed thickness dependences of $\Delta\varepsilon_1$ and f_1 behave qualitatively as $\Delta\varepsilon_{th} \sim d^2$ and $f_{th} \sim 1/d^2$, which can be estimated for the thickness mode [12]. In helicoidal samples the temperature dependences of $\Delta\varepsilon_1$ and f_1 below T_c differ from those expected for the Goldstone mode and thus they must reflect mostly the thickness mode behaviour. In fact these dependences are qualitatively similar to those in the 6 μm thick sample of **H6/9**, where only the thickness mode is present.

Mode 1 follows the Cole–Cole formula (equation (3)) with $\alpha_1 \sim 0{\cdot}1$. This relatively low value is quite understandable in the case of unwound samples, where this mode represents only the thickness mode. In helicoidal samples, where mode 1 is a superposition of two modes, such a low value of α can occur only when the relaxation

frequencies of both modes are not very different. A simple calculation shows that the value of $\alpha_1 \sim 0{\cdot}1$ is found for two modes of equal strength with relaxation frequencies f_r and $2f_r$ (see also [18]).

Mode 2, which was found only for **H6/9** at very low frequencies and is also thickness dependent, can be attributed to a mode connected with a non-homogeneous distribution of ionic space charge of low mobility, which might be localized preferentially near the sample surface. A similar mode has been also considered in ref. [8]. In contrast to ref. [8], we suggest that mode 2 is not only a dielectric mode, but that it is related to vibrations of the director, because it is detected in the electro-optical response as well.

Both modes 1 and 2, being strongly sample thickness dependent, do not represent bulk properties of the compounds studied as defined by material constants, but reflect the structure in real samples, which differ from the ideal one mainly owing to surface anchoring effects.

The authors are indebted to Drs V. Hamplová and M. Kašpar from this Institute for the liquid crystalline materials used in this study and to Dr I. Rychetský for valuable discussions on the relaxation modes. The work was supported by grants from The Grant Agency of the Czech Republic No. 202/96/1687 and 106/97/1337 and the grant COPERNICUS CP940168.

References

[1] Blinc, R., and Žekš, B., 1978, *Phys. Rev. A*, **18,** 740.
[2] Garoff, S., and Meyer, R. B., 1977, *Phys. Rev. Lett.*, **38,** 848.
[3] Carlsson, T., Žekš, B., Filipič, C., Levstik, A., and Blinc, R., 1988, *Mol. Cryst. liq. Cryst.*, **163,** 11.
[4] Beresnev, L. A., Pfeiffer, M., Pikin, S., Haase, W., and Blinov, L., 1992, *Ferroelectrics*, **132,** 99.
[5] Haase, W., Hiller, S., Pfeiffer, M., and Beresnev, L. A., 1993, *Ferroelectrics*, **140,** 34.
[6] Zubia, J., Ezcurra, A., De la Fuente, M. R., Pérez Jubindo, M. A., Sierra, T., and Serrano, J. L., 1991, *Liq. Cryst.*, **10,** 849.
[7] Ozaki, M., Nakao, K., Hatai, T., and Hoshino, K., 1989, *Liq. Cryst.*, **5,** 12.
[8] Uehara, H., Hanakai, Y., Hatano, J., Saito, S., and Murashiro, K., 1995, *Jpn. J. appl. Phys.*, **34,** 5424.
[9] Clark, N., and Lagerwall, S. T., 1980, *Appl. Phys. Lett.*, **36,** 899.
[10] Panarin, Yu, P., Kalmykov, Yu. P., Mac Lughadha, S. T., Xu, H., and Vij, J. K., 1994, *Phys. Rev. E*, **50,** 4763.
[11] Glogarová, M., and Pavel, J., 1984, *Mol. Cryst. liq. Cryst.*, **114,** 249.
[12] Glogarová, M., Sverenyák, H., Holakovský, J., Nguyen, H. T., and Destrade, C., 1995, *Mol. Cryst. liq. Cryst.*, **263,** 245.
[13] Miata, H., Maeda, M., and Suzuki, I., 1996, *Liq. Cryst.*, **20,** 303.
[14] Goodby, J. W., Slaney, A. J., Booth, C. J., Nishiyama, I., Vuijk, J. D., Styring, P., and Toyne, K. J., 1994, *Mol. Cryst. liq. Cryst.*, **234,** 231.
[15] Novotná, V., Glogarová, M., Sverenyák, H., and Bubnov, A. M., 16th ILCC Kent 1996, to be published in *Mol. Cryst. liq. Cryst.*
[16] Kašpar, M., Gorecka, E., Sverenyák, H., Hamplová, V., Glogarová, M., and Pakhomov, S. A., 1995, *Liq. Cryst.*, **19,** 589. In this reference the phase transition temperatures for **H6/9** slightly differ from those indicated in this paper; the reason is a different temperature calibration of the heating stages used.
[17] The synthesis and basic characteristics of these compounds will be published elsewhere.
[18] Liedermann, K., and Loidl, A., 1993, *J. non-cryst. Sol.*, **155,** 26.